Article:
Konijnenberg, A, Ranica, S, Narkiewicz, J et al. (4 more authors) (2016) Opposite Structural Effects of Epigallocatechin-3-gallate and Dopamine Binding to α-Synuclein. Analytical Chemistry, 88 (17). pp. 8468-8475. ISSN 0003-2700

https://doi.org/10.1021/acs.analchem.6b00731

Opposite structural effects of epigallocatechin-3-gallate and dopamine binding to α-synuclein

Albert Konijnenberg[1], Simona Ranica[2], Joanna Narkiewicz[3], Giuseppe Legname[3], Rita Grandori[2], Frank Sobott[1,4,5,*], and Antonino Natalello[2,6,*]

1) Biomolecular & Analytical Mass Spectrometry, University of Antwerp, Groenenborgerlaan 171, 2020 Antwerp, Belgium;

2) Department of Biotechnology and Biosciences, University of Milano-Bicocca, Piazza della Scienza 2, 20126 Milan, Italy;

3) Department of Neuroscience, Scuola Internazionale Superiore di Studi Avanzati (SISSA) and ELETTRA - Sincrotrone Trieste S.C.p.A, 34136 Trieste, Italy;

4) Astbury Centre for Structural Molecular Biology, University of Leeds, Leeds, LS2 9JT, UK;

5) School of Molecular and Cellular Biology, University of Leeds, Leeds, LS2 9JT, UK;

6) Consorzio Nazionale Interuniversitario per le Scienze Fisiche della Materia (CNISM), UdR of Milano-Bicocca, and Milan Center of Neuroscience (NeuroMI), 20126 Milan, Italy.

*Corresponding Authors

Frank Sobott, E-mail: frank.sobott@uantwerpen.be

Fax +32 3265 3233;

Antonino Natalello, E-mail: antonino.natalello@unimib.it

Fax +39 026448 3565.

ABSTRACT

The intrinsically disordered and amyloidogenic protein α-synuclein (AS) has been linked to several neurodegenerative states, including Parkinson's disease. Here, nano-electrospray-ionization mass spectrometry (nano-ESI-MS), ion mobility (IM), and native top-down electron transfer dissociation (ETD) techniques are employed to study AS interaction with small molecules known to modulate its aggregation, such as epigallocatechin-3-gallate (EGCG) and dopamine (DA). The complexes formed by the two ligands under identical conditions reveal peculiar differences. While EGCG engages AS in compact conformations, DA preferentially binds to the protein in partially extended conformations. The two ligands also have different effects on AS structure as assessed by IM, with EGCG leading to protein compaction and DA to its extension. Native top-down ETD on the protein-ligand complexes shows how the different observed modes of binding of the two ligands could be related to their known opposite effects on AS aggregation. The results also show that the protein can bind either ligand in the absence of any covalent modifications, such as e.g. oxidation.

KEYWORDS

Mass spectrometry, ion mobility, electron transfer dissociation, non-covalent complexes, Parkinson's disease, aggregation inhibitors, amyloid protein, intrinsically disordered protein.

INTRODUCTION

Amyloid aggregation of the intrinsically disordered protein (IDP) α-synuclein (AS) has been implicated in several neurodegenerative disorders, called synucleinopathies, including Parkinson's Disease (PD)[1]. In particular, AS is the major component of the Lewy Bodies (LB) from post-mortem brains of PD patients. Duplication, triplication and point mutations in the AS gene are associated with familial PD. AS is a highly abundant neuronal protein of 140 amino acids with an average molecular weight of 14460.1 Da. It exists in solution as a highly dynamic and heterogeneous conformational ensemble. The equilibrium between extended and partially folded conformations can be shifted by environmental factors and ligand binding. Solution pH, temperature, crowding agents, membranes, metal ions and interacting proteins have been shown to impact on AS conformational states[1]. Selective stabilization of distinct conformers is thought to elicit formation of supramolecular structures with different toxicities and amyloidogenic potentials[1].

Several classes of compounds, such as dyes, flavonoids, polyphenols and catecholamines, have been shown to inhibit AS fibrillation. Such inhibitors have attracted attention for the development of new drugs against amyloidoses[2,3]. A promising anti-amyloidogenic compound is the antioxidant molecule epigallocatechin-3-gallate (EGCG), the major green tea polyphenol which displays neuroprotective and anticancerogenic effects in cellular and animal models[4,5]. EGCG redirects AS aggregation into off-pathway, non-toxic, SDS-resistant, spherical and nanostructured oligomers of ~20-nm diameter[6]. Noteworthy, EGCG has been shown to affect in a similar way the aggregation pathway of several amyloidogenic proteins, such as Aβ[6], huntingtin[7] and ataxin-3[8]. Moreover, EGCG is capable of remodeling mature AS amyloid fibrils into smaller, non-toxic, amorphous aggregates[9]. Dopamine (DA) is among the most intensively studied modulators of AS-aggregation. A large amount of data substantiate the crucial role of DA and its oxidation products in PD[10], which is characterized by degeneration of dopaminergic neurons. In vivo, DA is synthesized in the cytosol of dopaminergic neurons where it is

stored in the monoaminergic vesicles and released in the intersynaptic space to interact with its physiological receptors[10-12]. DA has been shown to inhibit AS fibrillation and to promote aggregation into SDS-resistant oligomers[11]. It has been proposed that this process depends on DA oxidation but not on AS oxidation[13]. Other authors[14] suggested that the main mechanism of DA-dependent AS oligomerization is related to methionine oxidation. Moreover, it has been found that only a small fraction (5-10%) of AS is covalently binding DA oxidation products in the final aggregates obtained in vitro in the presence of the ligand, suggesting that DA and its oxidation products mainly act by non-covalent interactions[15]. DA-induced AS-oligomers have been associated to relatively low toxicity[16]. However, other works point to a well-defined toxicity with impairment of chaperone-mediated autophagy[17] and SNARE-mediated vesicle docking[18]. Electron micrographs show rod-shaped, nanostructured oligomers ~37 nm long[18]. It has been put forward that DA could serve as a lead molecular structure for the design of improved modulators[19].

The interaction of EGCG and DA with AS has been investigated by several biophysical methods[6,9,20-24], including native mass spectrometry[21-23]. Native mass spectrometry relies on gentle transfer of proteins and their complexes from solution into the gas phase of the mass spectrometer, without major structural rearrangements or disruption of non-covalent interactions[25-28]. As such it is especially useful for detecting non-covalent ligand binding[29,30]. However, a direct comparison of the complexes formed by AS with these two ligands has not been previously reported in the literature.

To better understand the molecular action of modulators of AS aggregation, the early stage of AS monomer interaction with EGCG and DA is investigated here by native MS, ion mobility, and native top-down electron transfer dissociation (ETD) in order to conjugate binding analysis to structural investigation. The two ligands display opposite conformational selectivity and distinct effects on AS compactness.

EXPERIMENTAL SECTION

Materials and sample preparation. See Supporting information**.**

Nano-ESI mass spectrometry. Mass spectrometry measurements were performed at a final protein concentration of 20 µM in 10 mM ammonium acetate pH 7.4. MS spectra were collected upon 10-min incubation of the protein-ligand mixtures at room temperature.

Nano-ESI-MS spectra were generally collected in positive-ion mode, using a hybrid quadrupole-time-of-flight mass spectrometer (QSTAR-Elite, Biosystems, Foster City, CA) equipped with a nano-ESI sample source. See the Supporting information for details.

Ion mobility. Ion mobility mass spectrometry (IM-MS) was performed on a Synapt G2 HDMS (Waters, Manchester, UK) using nano-ESI with homemade gold-coated borosilicate capillaries. Important settings were: 1.2-1.6 kV capillary voltage, 25 V sampling cone, 1 V extraction cone, 4 V trap CE, 0 V transfer CE, and 42 V trap bias. Gas pressures used throughout the instrument were 2.9 mbar, 2.4 E-2 mbar, 3.1 mbar and 2.6 E-2 mbar for the source, trap cell, IM cell and transfer cell respectively. Spectra were analyzed using Masslynx version 4.1 (Waters, Manchester, UK) and Driftscope v2.3 (Waters, Manchester, UK). Aggregate intensities per peak series (conformation) were extracted after a multiple Gauss curve fitting of the arrival time distributions based on the observed number of conformations. To identify relative intensities, the area under the fitted Gaussian curve of a single conformation was compared to the summed areas of all conformations.

Electron transfer dissociation. Native top-down MS experiments were performed using a Synapt G2 HDMS with ETD option. Important voltages were: sampling cone 25 V, extraction cone 1 V, trap collision energy 4 V, transfer collision energy 0.5-1 V and trap DC bias 40 V. Selected precursor ions (AS, AS+1DA and AS+1EGCG, all 12+ charge states for comparison) were mass-selected individually us-

ing the 32k quadrupole and underwent an ion-ion ETD reaction with 1,4 dicyanobenzene reagent in the trap T-wave (at ~5x10-2 mbar He) of the instrument. ETD settings used were a scan time interval of 1 s and a reagent refill time of 0.1 s. The wave velocity in the trap cell, where the ETD fragmentation takes place, was 300 m/s with a wave height of 0.4 V. ETD fragments were assigned manually.

RESULTS AND DISCUSSION

EGCG binding is observed preferentially with AS in compact conformations. The nano-ESI-MS spectrum of AS in the absence of the ligands (Fig. 1A) displays the typical multimodal charge-state distribution (CSD), with maxima at 8+ and 15+. Protein charge states in ESI-MS reflect the degree of structural compactness. Compact structures result in lower charge states, a feature that has been related to smaller solvent accessible surface area (SASA) and lower gas-phase basicity[31]. In agreement with previous reports[32,33], these results suggest coexistence of different conformational states for AS in solution at neutral pH with collapsed and extended conformers corresponding to the low- and high-charge envelope, respectively. Gaussian fitting of the CSD suggests the presence of a total of four components (Fig. S-1), which represent conformers of progressively increasing compactness as net charge decreases[32,33]. Small, dimer-specific peaks are also detectable (Fig. 1)[32].

Titration with EGCG leads to the appearance of protein-ligand complexes with up to 1:3 stoichiometry (Fig. 1A-D). The masses of the complexes in the mass-deconvoluted spectra (Fig. 1D) match within 2 Da tolerance with the theoretical values. The complexes can be dissociated by collisional activation, confirming the identity of the ligand and the non-covalent nature of the interaction (Fig. S-2 and S-3). Therefore, no protein or ligand oxidation, or other kind of covalent modification, is required for the initial establishment of AS-EGCG complexes.

It can be noted (Fig. 1B, 1C) that EGCG complexes are observed with higher relative intensity at low protein charge states, suggesting that this ligand either binds preferentially to AS in compact conforma-

tions or shifts the conformational equilibrium towards the compact state upon binding, or both. CSD analysis also shows that the low-charge component is progressively lost during the titration. This trend likely reflects selective depletion by aggregation into species that escape detection. Consistently, the total protein counts display a general trend of decrease along the titration, on the background of the experimental variability among runs (Fig. S-4). Thus, the net effect of these two phenomena is a minor shift of the average charge state along the titration (less than one unit).

To better illustrate the dependence of apparent binding affinity on charge state, Fig. 1E reports the total signal intensity of the AS-EGCG complexes (regardless of stoichiometry), relative to the signal intensity of the free protein, for the 8+ and 15+ charge states, representing the two maxima of the bimodal distribution. The results show higher fractions of bound protein for the 8+ ions (compact state) throughout the titration.

The signals of the free and bound protein can be extracted from the raw data and visualized separately for better comparison. The results are shown in Fig. S-5 for an intermediate point of the titration. It can be noted that the CSD of the bound form is shifted towards lower charge states relative to the CSD of the free protein, with a shift in average charge state from 14.1 to 13.1. Curve fitting performed selectively on the signals of either free or bound AS, in the presence of 80 µM EGCG, indicates a significant accumulation of the low-charge components (8.4 and 10.9) upon ligand binding, at the expense of the intermediate component (14.3) (Fig. S-6). The same comparison performed by combining all the stoichiometries $\geq$1 give similar results (data not shown). Altogether these results hint at structural differences in the conformational ensemble of free and EGCG-bound AS in solution, with increased average compactness of the bound protein.

Previous work has shown that EGCG binds more strongly to unfolded rather than folded proteins[6], consistent with an interaction with the polypeptide backbone. However, within the AS conformational ensemble, binding seems to involve preferentially compact species. These observations are not in conflict,

since the previously published analyses could not discriminate among different conformers of disordered ensembles. We performed additional measurements employing mixtures of AS, EGCG, and cytochrome c (CytC) as a reference protein to assess non-specific binding. As shown in Fig. S-7, CytC-EGCG complexes were detected in the ternary mixtures at similar levels as AS-EGCG complexes. Thus, the control experiment with a reference protein reveals non-specific binding of this ligand. This result is not unexpected, since EGCG has been reported to interact with a very large number of folded[34-40] and disordered[41,42] proteins. In particular, disorder-to-order transitions upon EGCG binding have been observed for the human salivary proline-rich protein IB5[41] and the dephosphorylated form of β-casein[42]. Moreover, EGCG has been shown to affect the aggregation pathway of several amyloidogenic proteins[4,6-8]. These studies also suggest that EGCG binds to the protein backbone, as well as to hydrophilic and hydrophobic side chains. The AS-EGCG interaction was also tested by nano-ESI-MS in negative-ion mode (Fig. S-8). In the absence of the ligand, AS displays a multimodal charge-state distribution[33], similar to positive-ion spectra. In the presence of the ligand, complexes are detected preferentially for the low-charge component (7- to 9-), resulting again in a shift of the CSD of the bound form towards lower charge states relative to the CSD of the free protein (Fig. S-8D). Also in this case, curve fitting performed selectively on the signals of either free or bound AS indicates a significant accumulation of the low-charge components (7.3 and 10.3) at the expenses of the intermediate component (13.9) upon ligand binding (Fig. S-8E and F). These results indicate that the observed trend does not depend on instrument polarity. This is the expected result for interactions characterized by real conformational selectivity and/or induced conformational changes, making less likely that the observed bias is due to artifacts of the electrospray process. These data also suggest that the applied experimental conditions do not affect the main structural features of the protein ensemble and the protein-ligand complexes.

EGCG binding promotes AS compaction. The structural effects of EGCG binding were further investigated by IM-MS. Native IM-MS is a gas phase separation technique where ions are separated based on their mobility in a gas filled drift tube upon applying a low electric field[43]. Their mobility is influenced by their compactness, mass and charge and thus even coexisting conformations of a protein with identical mass and charge can be separated[44,45]. The conformers populating each charge state are separated and characterized by their rotationally averaged collisional cross section (CCS)[46]. The IM-MS results are summarized in Fig. 2.

Multiple conformers were detected for low and intermediate charge state (6+ to 12+). Fig. 2A shows the change in relative populations of the 8+ charge state (with more extended conformations having a larger CCS) per EGCG bound state. Binding of EGCG progressively enhances AS compaction, increasing the relative amounts of the compact conformers as the number of EGCG molecules bound increases. EGCG binding does not yield new conformations, but rather shifts the conformational ensemble towards the two most compact states already present, although barely detectable, in the absence of the ligand. A comparison of the protein in the absence of ligand ("C" in Fig. 2A and B) with the unbound state in the presence of ligand ("0") shows largely the same conformational population, which is strong indication that no significant ligand loss occurs upon transfer from solution to the gas phase. Similar effects are observed for any of the charge states of AS displaying multiple conformations (Fig. S-9) independent of ionization mode (Fig. S-10). For charge states displaying only a single conformation, but where EGCG binding is observed (13+ to 15+), no conformational change is detected. It should be noted that high charge states are generally not very informative in IM experiments[46].

For CytC, too, IM measurements reveal more compact conformations upon increasing numbers of EGCG bound (Fig. S-11). In conclusion, these and previously published results point to EGCG as a generic binder[34-42] and modulator[41,42] of protein structure.

The protective effect of EGCG against amyloidosis has been attributed to the formation of off-pathway protein oligomers that prevent fibrillation[6]. The here reported results suggest that formation of these off-pathway species is preceded by a compaction of AS monomers upon EGCG binding. Compact conformations might interfere with on-pathway fibrillation in different ways. The compact monomers themselves might not be able to bind to existing β-sheet oligomers, thus preventing further elongation of proto-fibrils, and/or they could be sequestered into non-amyloidogenic, oligomeric structures[6].

DA binding is observed preferentially with AS in partially extended conformations. A typical AS titration with DA by nano-ESI-MS in positive-ion mode is shown in Fig. 3. The addition of the ligand leads to the appearance of AS:DA complexes, up to a 1:4 stoichiometry. The latter state however appears only at 6 mM DA concentrations and is only barely detectable (Fig. 3B). The identity of the ligand and the absence of covalent modifications have been confirmed by dissociation of the non-covalent complexes in MS/MS experiments (Fig. S-12). All the masses of the parent and product ions in the MS/MS spectra (Fig. 3B and S-12) match the theoretical values within 1.3 Da tolerance.

Complexes are detected preferentially for the protein charge states 10+ to 17+ (Fig. 3A), corresponding to partially extended conformations of AS monomers (Fig. S-1). To better illustrate this trend, Fig. 3C reports the relative intensity of free and bound protein for the 8+ and 15+ charge states, as shown above for EGCG. The results show a strong bias in favor of the highly charged ions. These data are in agreement with previous MS analyses of these complexes[21,22]. The extracted CSDs of the free and bound protein for an intermediate point of the titration are reported in Fig. S-13. The results show a shift towards intermediate charge states for the bound form, with increasing intensity for the 12+ and 13+ ions and decreasing intensity for all the other charge states. The same comparison performed by combining all the stoichiometries $\geq$1 gives similar results (data not shown). Curve fitting performed selectively on the signals of either free or bound AS, in the presence of 200 μM DA, (Fig. S-14) indicates a signifi-

cant accumulation of the intermediate component (13.4) at the expenses of the high- and low-charge components upon ligand binding (Fig. S-14).

The results at 6 mM DA are compared with the occupancy profiles predicted by protein-ligand binding models with identical and independent interaction sites, assuming either a 1:3 or a 1:4 stoichiometry (Fig. 3D). The data fit the 1:3 model better, with some minor additional non-specific binding leading to the appearance of very small amounts of the 1:4 complex. These results suggest that AS contains three non-cooperative binding sites for DA. The same analysis of the data obtained at 500 µM DA does not discriminate between the two alternative models (Fig. S-15). Ternary mixtures with CytC as a reference protein confirm that non-specific DA binding is negligible (Fig. S-16). Also in such mixtures (as expected) DA binding to AS was observed preferentially with partially extended conformations.

Measurements in the negative-ion mode failed to detect AS-DA complexes, although free, deprotonated DA can be detected in the spectra (data not shown). Therefore, additional control experiments were performed by measurements in positive-ion mode. Tyrosine, which is structurally similar to DA but does not affect AS fibrillation[13], was used as a negative control. Different from DA, tyrosine forms detectable complexes only at mM concentrations. The data obtained with 1 mM DA or tyrosine are shown in Fig. S-16 for comparison, showing much stronger binding by DA. The free ligand concentrations corresponding to 50% saturation [47] are 438.4 µM ± 90.8µM for DA and 3.51 mM ± 0.84 mM for Tyr. The value obtained for DA is of the same order of magnitude as the recently reported dissociation constant by isothermal titration calorimetry (285 µM)[20], although quite a broad range of values are reported in the literature[24,48]. Furthermore, Tyr binding does not induce changes in the CSD comparable to those observed with DA (Fig. S-17). Thus, the evidence of a bias for intermediate charge states, defined stoichiometry, and different responses to DA and tyrosine suggests that the observed complexes reflect, indeed, AS binding propensities characteristic of the solution phase, rather than adduct formation induced by the electrospray conditions. The lack of complexes in negative-ion mode might be

due to enrichment of deprotonated DA inside the ESI droplets, which could in turn represent a poor ligand for AS[19].

DA binding promotes AS elongation. IM-MS was used to investigate structural effects of DA binding to AS. Similar to EGCG, DA binding affects the equilibrium among conformations present already in the free protein (Fig. 2C and D). With increasing numbers of DA bound, the 11+ charge state of AS becomes increasingly extended (Fig. 2C). Similar results are obtained for the 10+ and 12+ CS, which all display two coexisting conformations for unbound AS. From CS 13+ and higher, AS exists in a single conformation in the gas phase, which does not change significantly upon DA binding (Fig. S-18). Given that DA is positively charged at neutral pH and likely binds as a protonated species to AS in positive-ion mode, it might be argued that the observed effect of DA on AS structure is due to electrostatic repulsions peculiar to the gas phase. However, it should be noted that CCS variations are detected here within a given charge state. Thus, comparison is performed always among ions with the same net charge, and the observed changes in drift time are interpreted as a specific structural effect, linked to the nature of the ligand. It could be also argued that the more extended conformers accumulating at increasing DA loading derive from higher charge state(s) by loss of charged ligand molecule(s) and retention of the conformation typical of the higher charge state. However, such a mechanism would be expected to produce the more extended conformer also in the "empty" protein, by dissociation of the ligand from the 1:1 complex, which is not the case here. Furthermore, structures would be expected to rearrange upon charge reduction[49]. Recently, conformational studies on IDPs by ESI-MS and ESI-IM-MS have been questioned[50]. In particular, the compact components frequently detected by these techniques have been ascribed to the electrospray process itself. Multiple competing mechanisms for the release of the IDP from the droplet would cause the multiple overlapping CSDs which are often observed for IDPs. Interestingly, the effects reported here on the CSDs and CCSs of a single protein are ligand-

specific and have opposite directions, making it unlikely that they merely reflect consequences of the electrospray mechanism.

As dopaminergic neuron loss is a hallmark of PD and clinical symptoms can be alleviated by administering L-dopa, the DA metabolism has been linked to AS aggregation. Our results suggest that at least the initial interaction between AS and DA is of a specific, noncovalent nature. In addition, there is no need for modification of AS or DA, such as oxidation of AS or conversion of DA to melanin or other oxidation products, to establish this interaction. Although these results do not rule out that such interactions exist and can contribute to toxicity, the initial effect of dopamine binding seems to be elongation of AS monomers. Initial DA-dependent elongation of AS might well fit to a model where AS oligomerization is achieved through stacking of extended monomers without any end-to-end associations[51], which are eventually cross-linked with DA-quinone/DA-melanin oxidation products. As such, DA binding might already prime AS for off-pathway oligomerization[52].

Correlating the structure remodeling by DA and EGCG with their binding modes. To assess whether we could correlate the structural remodeling effect of DA and EGCG to their modes of binding, we turned to ETD ligand footprinting on free AS as well as the DA- and EGCG-bound complexes. Top-down electron transfer dissociation (ETD) experiments are based on sequencing intact proteins with a radical-driven fragmentation method combined with mass spectrometry detection yielding information on the primary structure of the protein with amino acid resolution[53,54]. As ETD primarily cleaves the backbone of the protein, it maintains most non-covalent interactions, such as ligand binding or higher order protein structure when performed on native proteins[55-57]. As we have shown that both the DA and EGCG interactions are non-covalent, it is important to perform native top-down ETD to prevent disruption of these labile interactions and to accurately determine their binding sites. The results of these experiments are summarized in Fig. 4 and show a reasonable sequence coverage for free AS (42 %), in line with previously observed fragmentation efficiency of AS[58]. Upon exposing the 1:1

non-covalent AS-ligand complexes to native ETD, we see a slight increase in sequence coverage (49% and 44% for DA and EGCG, respectively), which is caused by peptides that are ligand-bound. The DA binding site was located in the C-terminal amino acids $_{127}$MPSEE$_{131}$. Indeed binding of DA to AS has been reported near the $_{125}$YEMPS$_{129}$ region[59], which overlaps with the binding site observed by top-down ETD. The localization of M_{127} within this region is interesting as it might explain the mechanism by which DA prevents fibril formation and induces DA-dependent oligomerization. The localization of a well-defined binding site near this methionine would facilitate oxidation of M_{127}, which in turn has been coined to be crucial for disruption of fibril formation by redirecting oligomerization of AS into off-pathway species[14,52,60]. The series of fragments from the $_{98}$DQLGKN$_{103}$ stretch could confirm previous observations by molecular modelling that apart from binding the $_{125}$YEMPS$_{129}$ region, DA also shows interactions with residues near the NAC domain of AS, thus promoting fragmentation in this region[61].

The fragmentation pattern for the AS-EGCG complex reveals partial binding and not well localized, as peptide fragments carrying EGCG were found across the protein sequence together with their unbound counterparts. These results strengthen the conclusions about non-specific binding of EGCG to the peptide backbone. The absence of a well-defined binding site is interesting as it shows how an effective modulator of aggregation can utilize non-specific rather than specific binding. The ability of compounds like EGCG that bind non-specifically but can direct the conformational ensemble in a specific direction might be a novel and potent method to affect structurally promiscuous drug targets.

CONCLUSIONS

This work shows for the first time that EGCG and DA have opposite structural effects on AS conformational ensembles. This effect is consistently shown by CSD analysis, which is supposed to capture

the state of the protein at the time of leaving the solution, and by IM measurements, which depict structures in the gas phase.

These findings help to rationalize the previously reported differences between the two ligands on AS aggregation (Fig. 5). Both DA and EGCG are known to stabilize AS oligomers. However, while DA-induced oligomers display some toxicity on cultured cells[16-18], EGCG-induced oligomers are non-toxic[6]. The accumulation of compact or elongated protein-ligand complexes in the presence of the different ligands is likely at the basis of their distinct effects on AS aggregation mechanism.

Preferential binding to specific conformers of amyloid proteins has recently been reported for inhibitors of the fibrillation pathway of β2-microglobulin[62] and amylin[63]. This study further underscores the potential use of ESI-MS, ion mobility and native top-down ETD for the investigation of protein-inhibitor interactions and for drug screening[64-66]. The interplay among ligand-binding, oxidation, AS oligomerization and aggregation is still not completely understood. The data reported here indicate that covalent modifications of EGCG, DA, and AS are not required in order to establish interactions of the protein with the ligands and to induce structural changes in the protein. These results demonstrate the power of nano-ESI-IM-MS in investigating the mechanism of action of potential anti-fibrillogenic compounds, thanks to the possibility to retrieve combined information on conformational properties and binding state of proteins in heterogeneous mixtures.

ASSOCIATED CONTENT

Supporting Information Available: supporting information for the EXPERIMENTAL SECTION (materials and sample preparation and nano-ESI-MS analysis), 18 supporting figures and 8 supplementary references. This material is available free of charge via the Internet at http://pubs.acs.org.

AUTHOR INFORMATION

Corresponding Authors

*E-mail: frank.sobott@uantwerpen.be

*E-mail: antonino.natalello@unimib.it

Author contributions

G.L., R.G., F.S. and A.N. conceived the study; J.N. produced the recombinant protein; A.N. performed the nano-ESI-MS analysis; A.K. and S.R. performed the IM analysis; A.K. performed the ETD analysis; A.K., F.S., R.G. and A.N. wrote the manuscript; all authors have read and approved the manuscript.

Notes

The authors declare no competing financial interests.

ACKNOWLEDGMENT

This work was supported by the grant 12-1-2001100-148 from the University of Milano-Bicocca (Fondo di Ateneo per la Ricerca). The authors would like to thank the Hercules foundation for funding of the Synapt G2 instrument.

REFERENCES

(1) Breydo, L.; Wu, J. W.; Uversky, V. N. Biochim. Biophys. Acta. **2012**, 1822, 261-285.

(2) Narkiewicz, J.; Giachin, G.; Legname, G. Prion **2014**, 8, 19-32.

(3) Masuda, M.; Suzuki, N.; Taniguchi, S.; Oikawa, T.; Nonaka, T.; Iwatsubo, T.; Hisanaga, S. I.; Goedert, M.; Hasegawa, M. Biochemistry **2006**, 45, 6085-6094.

(4) Cheng, B.; Gong, H.; Xiao, H.; Petersen, R. B.; Zheng, L.; Huang, K. Biochim. Biophys. Acta. **2013**, 1830, 4860-4871.

(5) Singh, B. N.; Shankar, S.; Srivastava, R. K. Biochem. Pharmacol. **2011**, 82, 1807-1821.

(6) Ehrnhoefer, D. E.; Bieschke, J.; Boeddrich, A.; Herbst, M.; Masino, L.; Lurz, R.; Engemann, S.; Pastore, A.; Wanker, E. E. Nat. Struct. Mol. Biol. **2008**, 15, 558-566.

(7) Ehrnhoefer, D. E.; Duennwald, M.; Markovic, P.; Wacker, J. L.; Engemann, S.; Roark, M.; Legleiter, J.; Marsh, J. L.; Thompson, L. M.; Lindquist, S.; Muchowski, P. J.; Wanker, E. E. Hum. Mol. Genet. **2006**, 15, 2743-2751.

(8) Bonanomi, M.; Natalello, A.; Visentin, C.; Pastori, V.; Penco, A.; Cornelli, G.; Colombo, G.; Malabarba, M. G.; Doglia, S. M.; Relini, A.; Regonesi, M. E.; Tortora, P. Hum. Mol. Genet. **2014**, 23, 6542-6552.

(9) Bieschke, J.; Russ, J.; Friedrich, R. P.; Ehrnhoefer, D. E.; Wobst, H.; Neugebauer, K.; Wanker, E. E. Proc. Natl. Acad. Sci. USA **2010**, 107, 7710-7715.

(10) Venda, L. L.; Cragg, S. J.; Buchman, V. L.; Wade-Martins, R. Trends Neurosci. **2010**, 33, 559-568.

(11) Leong, S. L.; Cappai, R.; Barnham, K. J.; Pham, C. L. L. Neurochem. Res. **2009**, 34, 1838-1846.

(12) Bisaglia, M.; Filograna, R.; Beltramini, M.; Bubacco, L. Ageing Res. Rev. **2014**, 13, 107-114.

(13) Norris, E. H.; Giasson, B. I.; Hodara, R.; Xu, S. H.; Trojanowski, J. Q.; Ischiropoulos, H.; Lee, V. M. Y. J. Biol. Chem. **2005**, 280, 21212-21219.

(14) Leong, S. L.; Pham, C. L. L.; Galatis, D.; Fodero-Tavoletti, M. T.; Perez, K.; Hill, A. F.; Masters, C. L.; Ali, F. E.; Barnham, K. J.; Cappai, R. Free Radic. Biol. Med. **2009**, 46, 1328-1337.

(15) Bisaglia, M.; Tosatto, L.; Munari, F.; Tessari, I.; de Laureto, P. P.; Mammi, S.; Bubacco, L. Biochem. Biophys. Res. Commun. **2010**, 394, 424-428.

(16) Pieri, L.; Madiona, K.; Melki, R. Sci. Rep. **2016**, 6:24526.

(17) Martinez-Vicente, M.; Talloczy, Z.; Kaushik, S.; Massey, A. C.; Mazzulli, J.; Mosharov, E. V.; Hodara, R.; Fredenburg, R.; Wu, D. C.; Follenzi, A.; Dauer, W.; Przedborski, S.; Lschiropoulos, H.; Lansbury, P. T.; Sulzer, D.; Cuervo, A. M. J. Clin. Invest. **2008**, 118, 777-788.

(18) Choi, B. K.; Choi, M. G.; Kim, J. Y.; Yang, Y.; Lai, Y.; Kweon, D. H.; Lee, N. K.; Shin, Y. K. Proc. Natl. Acad. Sci. USA **2013**, 110, 4087-4092.

(19) Latawiec, D.; Herrera, F.; Bek, A.; Losasso, V.; Candotti, M.; Benetti, F.; Carlino, E.; Kranjc, A.; Lazzarino, M.; Gustincich, S.; Carloni, P.; Legname, G. PLoS ONE **2010**, 5(2): e9234.

(20) Tavassoly, O.; Nokhrin, S.; Dmitriev, O. Y.; Lee, J. S. FEBS J. **2014**, 281, 2738-2753.

(21) Illes-Toth, E.; Dalton, C. F.; Smith, D. P. J. Am. Soc. Mass Spectrom. **2013**, 24, 1346-1354.

(22) Shimotakahara, S.; Shiroyama, Y.; Fujimoto, T.; Akai, M.; Onoue, T.; Seki, H.; Kado, S.; Machinami, T.; Shibusawa, Y.; Uéda, K.; Tashiro, M. J. Biophys. Chem. **2012**, 3, 149-155.

(23) Liu, Y. Q.; Ho, L. H.; Carver, J. A.; Pukala, T. L. Aust. J. Chem. **2011**, 64, 36-40.

(24) Corvaglia, S.; Sanavio, B.; Hong Enriquez, R. P.; Sorce, B.; Bosco, A.; Scaini, D.; Sabella, S.; Pompa, P. P.; Scoles, G.; Casalis, L. Sci. Rep. **2014**, 4:5366.

(25) Konijnenberg, A.; Butterer, A.; Sobott, F. Biochim. Biophys. Acta **2013**, 1834, 1239-1256.

(26) Hilton, G. R.; Benesch, J. L. P. J. R. Soc. Interface **2012**, 9, 801-816.

(27) Lorenzen, K.; van Duijn, E. Curr. Protoc. Protein Sci. **2010**, (SUPPL.62), art. no. 17.12.

(28) Sobott, F.; McCammon, M. G.; Hernández, H.; Robinson, C. V.; Karplus, M.; Dobson, C. M.; Scoles, G.; Zewail, A. H.; McMillan, P. F.; Finney, J. L. Philos. Trans. A: Math. Phys. Eng. Sci. **2005**, 363, 379-391.

(29) Sharon, M.; Horovitz, A. Curr. Opin. Struct. Biol. **2015**, 34, 7-16.

(30) Schmidt, C.; Robinson, C. V. FEBS J. **2014**, 281, 1950-1964.

(31) Li, J.; Santambrogio, C.; Brocca, S.; Rossetti, G.; Carloni, P.; Grandori, R. Mass Spectrom. Rev. **2016**, 35, 111-122.

(32) Frimpong, A. K.; Abzatimov, R. R.; Uversky, V. N.; Kaltashov, I. A. Proteins **2010**, 78, 714-722.

(33) Natalello, A.; Benetti, F.; Doglia, S. M.; Legname, G.; Grandori, R. Proteins **2011**, 79, 611-621.

(34) Ognjenović, J.; Stojadinović, M.; Milčić, M.; Apostolović, D.; Vesić, J.; Stambolić, I.; Atanasković-Marković, M.; Simonović, M.; Velickovic, T. C. Food Chem. **2014**, 164, 36-43.

(35) Wu, X.; He, W.; Yao, L.; Zhang, H.; Liu, Z.; Wang, W.; Ye, Y.; Cao, J. J. Agric. Food Chem. **2013**, 61, 8829-8835.

(36) Pelaez-Aguilar, A. E.; Rivillas-Acevedo, L.; French-Pacheco, L.; Valdes-Garcia, G.; Maya-Martinez, R.; Pastor, N.; Amero, C. Biochemistry **2015**, 54, 4978-4986.

(37) Miyata, M.; Sato, T.; Kugimiya, M.; Sho, M.; Nakamura, T.; Ikemizu, S.; Chirifu, M.; Mizuguchi, M.; Nabeshima, Y.; Suwa, Y.; Morioka, H.; Arimori, T.; Suico, M. A.; Shuto, T.; Sako, Y.; Momohara, M.; Koga, T.; Morino-Koga, S.; Yamagata, Y.; Kai, H. Biochemistry **2010**, 49, 6104-6114.

(38) Bonanomi, M.; Visentin, C.; Natalello, A.; Spinelli, M.; Vanoni, M.; Airoldi, C.; Regonesi, M. E.; Tortora, P. Chemistry **2015**, 21, 18383-18393.

(39) Williamson, M. P.; McCormick, T. G.; Nance, C. L.; Shearer, W. T. J. Allergy Clin. Immunol. **2006**, 118, 1369-1374.

(40) Menegazzi, M.; Mariotto, S.; Dal Bosco, M.; Darra, E.; Vaiana, N.; Shoji, K.; Safwat, A. A.; Marechal, J. D.; Perahia, D.; Suzuki, H.; Romeo, S. FEBS J. **2014**, 281, 724-738.

(41) Canon, F.; Ballivian, R.; Chirot, F.; Antoine, R.; Sarni-Manchado, P.; Lemoine, J.; Dugourd, P. J. Am. Chem. Soc. **2011**, 133, 7847-7852.

(42) Jöbstl, E.; O'Connell, J.; Fairclough, J. P. A.; Williamson, M. P. Biomacromolecules **2004**, 5, 942-949.

(43) Dugourd, P.; Hudgins, R. R.; Clemmer, D. E.; Jarrold, M. F. Rev. Sci. Instrum. **1997**, 68, 1122-1129.

(44) Uetrecht, C.; Rose, R. J.; Van Duijn, E.; Lorenzen, K.; Heck, A. J. R. Chem. Soc. Rev. **2010**, 39, 1633-1655.

(45) Lanucara, F.; Holman, S. W.; Gray, C. J.; Eyers, C. E. Nat. Chem. **2014**, 6, 281-294.

(46) Jurneczko, E.; Barran, P. E. Analyst **2011**, 136, 20-28.

(47) Sun, J. X.; Kitova, E. N.; Wang, W. J.; Klassen, J. S. Anal. Chem. **2006**, 78, 3010-3018.

(48) Cappai, R.; Leck, S. L.; Tew, D. J.; Williamson, N. A.; Smith, D. P.; Galatis, D.; Sharples, R. A.; Curtain, C. C.; Ali, F. E.; Cherny, R. A.; Culvenor, J. G.; Bottomley, S. P.; Masters, C. L.; Barnham, K. J.; Hill, A. F. FASEB J. **2005**, 19, 1377-1379.

(49) Lermyte, F.; Łącki, M. K.; Valkenborg, D.; Gambin, A.; Sobott, F. J. Am. Soc. Mass Spectrom. **2016**, in press.

(50) Borysik, A. J.; Kovacs, D.; Guharoy, M.; Tornpa, P. J. Am. Chem. Soc. **2015**, 137, 13807-13817.

(51) Rekas, A.; Knott, R. B.; Sokolova, A.; Barnham, K. J.; Perez, K. A.; Masters, C. L.; Drew, S. C.; Cappai, R.; Curtain, C. C.; Pham, C. L. L. Eur. Biophys. J. **2010**, 39, 1407-1419.

(52) Conway, K. A.; Rochet, J. C.; Bieganski, R. M.; Lansbury, P. T. Science **2001**, 294, 1346-1349.

(53) Mikesh, L. M.; Ueberheide, B.; Chi, A.; Coon, J. J.; Syka, J. E. P.; Shabanowitz, J.; Hunt, D. F. Biochim. Biophys. Acta. **2006**, 1764, 1811-1822.

(54) Syka, J. E. P.; Coon, J. J.; Schroeder, M. J.; Shabanowitz, J.; Hunt, D. F. Proc. Natl. Acad. Sci. USA **2004**, 101, 9528-9533.

(55) Clarke, D. J.; Murray, E.; Hupp, T.; MacKay, C. L.; Langridge-Smith, P. R. R. J. Am. Soc. Mass Spectrom. **2011**, 22, 1432-1440.

(56) Lermyte, F.; Konijnenberg, A.; Williams, J. P.; Brown, J. M.; Valkenborg, D.; Sobott, F. J. Am. Soc. Mass Spectrom. **2014**, 25, 343-350.

(57) Lermyte, F.; Sobott, F. Proteomics **2015**, 15, 2813-2822.

(58) Xie, Y.; Zhang, J.; Yin, S.; Loo, J. A. J. Am. Chem. Soc. **2006**, 128, 14432-14433.

(59) Herrera, F. E.; Chesi, A.; Paleologou, K. E.; Schmid, A.; Munoz, A.; Vendruscolo, M.; Gustincich, S.; Lashuel, H. A.; Carloni, P. PLoS ONE **2008**, 3 (10):e3394.

(60) Nakaso, K.; Tajima, N.; Ito, S.; Teraoka, M.; Yamashita, A.; Horikoshi, Y.; Kikuchi, D.; Mochida, S.; Nakashima, K.; Matsura, T. PLoS ONE **2013**, 8 (2):e55068.

(61) Dibenedetto, D.; Rossetti, G.; Caliandro, R.; Carloni, P. Biochemistry **2013**, 52, 6672-6683.

(62) Woods, L. A.; Platt, G. W.; Hellewell, A. L.; Hewitt, E. W.; Homans, S. W.; Ashcroft, A. E.; Radford, S. E. Nat. Chem. Biol. **2011**, 7, 730-739.

(63) Young, L. M.; Cao, P.; Raleigh, D. P.; Ashcroft, A. E.; Radford, S. E. J. Am. Chem. Soc. **2013**, 136, 660-670.

(64) Young, L. M.; Saunders, J. C.; Mahood, R. A.; Revill, C. H.; Foster, R. J.; Tu, L.-H.; Raleigh, D. P.; Radford, S. E.; Ashcroft, A. E. Nat. Chem. **2015**, 7, 73-81.

(65) Young, L. M.; Saunders, J. C.; Mahood, R. A.; Revill, C. H.; Foster, R. J.; Ashcroft, A. E.; Radford, S. E. Methods **2016**, 95, 62-69.

(66) Woods, L. A.; Radford, S. E.; Ashcroft, A. E. Biochim. Biophys. Acta. **2013**, 1834, 1257-1268.

FIGURE CAPTIONS

Figure 1. Detection of AS-EGCG complexes by MS. (A) Nano-ESI-MS spectra in positive-ion mode for a titration of 20 μM AS by increasing EGCG concentrations. (B, C) Magnification of selected spectra (0 and 100 μM EGCG) of (A) in the 900-1100 (B) and 1600-2100 (C) m/z regions. The number of EGCG molecules bound to AS monomers is indicated by red numbers. Dimer-specific peaks of AS are labeled as "D". The ammonium adduct of the EGCG dimer is labeled as "D*" (almost overlapped to the 1:1 complex). (D) Deconvolution of selected spectra (0 and 100 μM EGCG) of (A). (E) Intensity of the AS-EGCG complexes (regardless of stoichiometry) for the 8+ and the 15+ ions, relative to the total ion intensity of each charge state, as a function of EGCG concentration. Error bars represent the standard deviation from three independent experiments.

Figure 2. IM-MS reveals an opposite conformational effect of EGCG and DA binding to AS monomers. (A, B) Heat maps of the conformations detected for the 8+ and 15+ charge state of AS, as a function of the number of EGCG bound molecules. (C, D) Heat maps of the conformations detected for the 11+ and 15+ charge state of AS, as a function of the number of DA bound molecules. C, control sample in the absence of the ligand.

Figure 3. Detection of AS-DA complexes by MS. (A) Nano-ESI-MS spectra in positive-ion mode for a titration of 20 μM AS by increasing DA concentrations. AS dimer-specific peaks are labeled as "D". The number of DA molecules bound to AS monomers is indicated by red numbers, for selected peaks. (B) Deconvoluted spectra of the data reported in (A). (C) Relative intensity of the AS-DA complexes (regardless of stoichiometry) versus total ion intensity for each charge state are reported for different DA concentrations for the 8+ (compact AS monomers) and 15+ (AS extended conformation) ions. (D) Species distribution of AS-DA complexes of distinct stoichiometry as derived from the measurements

at 20 µM AS and 6 mM DA. The values calculated according to the 1:3 and 1:4 models, assuming identical and independent binding sites, are reported, too. Error bars represent the standard deviation from three independent experiments.

Figure 4. Native top-down ETD reveals binding regions for DA and EGCG. Sequence coverage for AS in absence (top) and presence of the ligands DA (middle) and EGCG (bottom). Blue brackets indicate either c or z fragments without ligand bound, whereas red brackets mark fragments that maintain an interaction with the ligand. For DA a well defined binding site within the AS $_{125}$YEMPS$_{129}$ region was observed, whereas for EGCG a more scattered pattern was observed in line with non-specific binding.

Figure 5. Model for the mechanism of action by EGCG and DA on AS aggregation. Under normal conditions, AS exists as a mixture of several conformational states characterized by different compactness. Distinct aggregation pathways may be triggered by environmental factors capable of shifting the conformational equilibrium towards peculiar aggregation-prone conformers. EGCG leads to the accumulation of complexes with AS in compact conformations, while DA leads to extended protein-ligand complexes. The opposite behavior of the two compounds is expected to yield AS aggregates with different structural properties and toxicities.

FIGURES

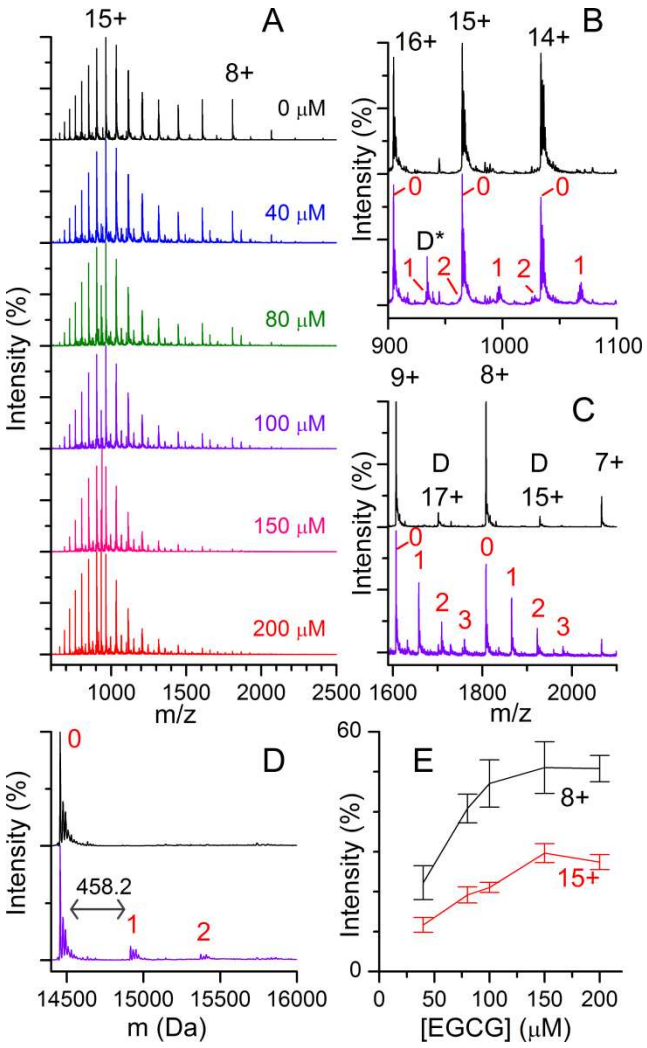

Figure 1

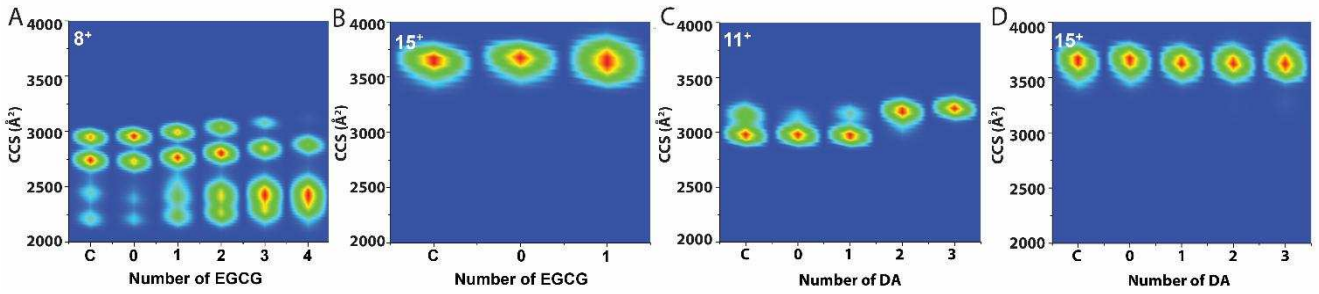
A
8+
CCS (Å²)
4000
3500
3000
2500
2000
C 0 1 2 3 4
Number of EGCG
B
15+
C 0 1
Number of EGCG
C
11+
C 0 1 2 3
Number of DA
D
15+
C 0 1 2 3
Number of DA

Figure 2

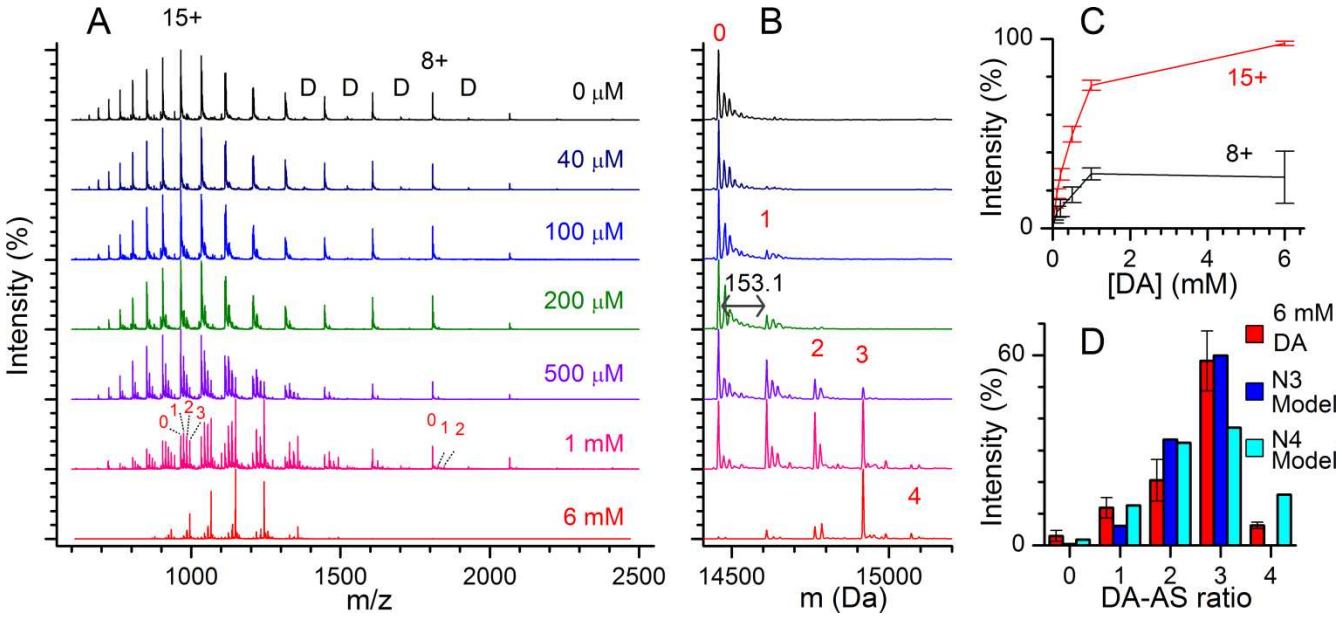
A
15+
8+
D
D
D
D
0 μM
40 μM
100 μM
200 μM
500 μM
1 mM
6 mM
Intensity (%)
m/z
B
0
1
153.1
2
3
4
m (Da)
C
100
0
15+
8+
Intensity (%)
[DA] (mM)
D
60
0
6 mM DA
N3 Model
N4 Model
Intensity (%)
DA-AS ratio

Figure 3

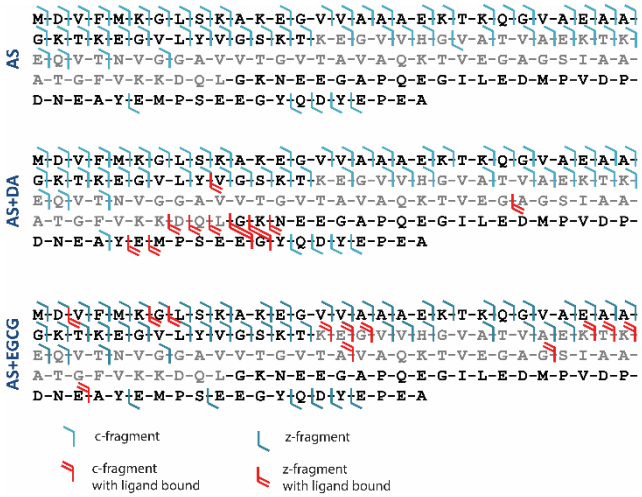
AS
AS+DA
AS+EGCG
c-fragment
z-fragment
c-fragment with ligand bound
z-fragment with ligand bound

Figure 4

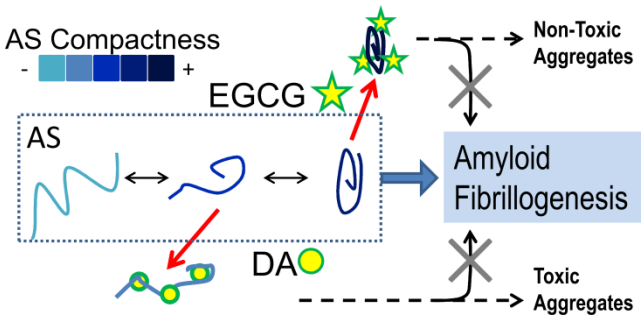
AS Compactness
-
+
EGCG
AS
DA
Amyloid
Fibrillogenesis
Non-Toxic
Aggregates
Toxic
Aggregates

Figure 5

for TOC only